First determination of the CP content of $D \to \pi^+\pi^-\pi^+\pi^-$ and improved determination of the CP contents of $D \to \pi^+\pi^-\pi^0$ and $D \to K^+K^-\pi^0$

S. Malde[a], C. Thomas[a], G. Wilkinson[a,b], C. Prouve[c], J. Rademacker[c], J. Libby[d], M. Nayak[d], T. Gershon[e]

[a] *University of Oxford, Denys Wilkinson Building, Keble Road, OX1 3RH, United Kingdom*
[b] *European Organisation for Nuclear Research (CERN), CH-1211, Geneva 23, Switzerland*
[c] *University of Bristol, Bristol, BS8 1TL, United Kingdom*
[d] *Indian Institute of Technology Madras, Chennai 600036, India*
[e] *University of Warwick, Coventry, CV4 7AL, United Kingdom*

Abstract

Quantum-correlated $\psi(3770) \to D^0\overline{D}^0$ decays collected by the CLEO-c experiment are used to perform a first measurement of $F_+^{4\pi}$, the fractional CP-even content of the self-conjugate decay $D \to \pi^+\pi^-\pi^+\pi^-$, obtaining a value of 0.737 ± 0.028. An important input to the measurement comes from the novel use of $D \to K^0_S\pi^+\pi^-$ and $D \to K^0_L\pi^+\pi^-$ decays to tag the signal mode. This same technique is applied to the channels $D \to \pi^+\pi^-\pi^0$ and $D \to K^+K^-\pi^0$, yielding $F_+^{\pi\pi\pi^0} = 1.014 \pm 0.045 \pm 0.022$ and $F_+^{KK\pi^0} = 0.734 \pm 0.106 \pm 0.054$, where the first uncertainty is statistical and the second systematic. These measurements are consistent with those of an earlier analysis, based on CP-eigenstate tags, and can be combined to give values of $F_+^{\pi\pi\pi^0} = 0.973 \pm 0.017$ and $F_+^{KK\pi^0} = 0.732 \pm 0.055$. The results will enable the three modes to be cleanly included in measurements of the unitarity triangle angle γ using $B^\mp \to DK^\mp$ decays, and in time-dependent studies of CP violation and mixing in the $D^0\overline{D}^0$ system.

Keywords: charm decay, quantum correlations, CP violation

1. Introduction

Studies of the process $B^{\mp} \to DK^{\mp}$, where D indicates a neutral charmed meson reconstructed in a state accessible to both D^0 and $\overline{D}^0$ decays, give sensitivity to the unitarity triangle angle $\gamma \equiv \arg(-V_{\rm ud}V_{\rm ub}^*/V_{\rm cd}V_{\rm cb}^*)$ (also denoted ϕ_3). Improved knowledge of γ is necessary for testing the Standard Model description of *CP* violation. In a recent publication [1] it was shown how inclusive three-body self-conjugate D meson decays can be used for this purpose, provided their fractional *CP*-even content is known, a quantity denoted F_+ (or F_+^f when it is necessary to designate the specific decay f). Measurements of F_+ for the decays $D \to \pi^+\pi^-\pi^0$ and $D \to K^+K^-\pi^0$ were performed, making use of quantum-correlated $D^0\overline{D}^0$ decays coherently produced at the $\psi(3770)$ resonance and collected by the CLEO-c detector. In this Letter a first measurement is presented of the *CP* content of the four-body mode $D \to \pi^+\pi^-\pi^+\pi^-$, again exploiting CLEO-c $\psi(3770)$ data. This fully-charged and relatively abundant final state [2] can be reconstructed with good efficiency by the LHCb detector and hence is a promising mode for improving the determinaton of γ at that experiment, as well as at Belle II.

The three-body analysis reported in Ref. [1] exploited events in which one D meson is reconstructed in the signal mode and the other 'tagging' meson in its decay to a *CP* eigenstate. The measurement of $F_+^{4\pi}$ presented in this Letter follows the same method, but augments it with other approaches, in particular a powerful new strategy in which the tagging modes are $D \to K^0_{\rm S,L}\pi^+\pi^-$, and attention is paid to where on the Dalitz plot this tag decay occurs. In order to benefit from this strategy for the previously studied decays, this Letter also presents measurements of $F_+^{\pi\pi\pi^0}$ and $F_+^{KK\pi^0}$ using $D \to K^0_{\rm S,L}\pi^+\pi^-$ tags. Throughout the effects of *CP* violation in the charm system are neglected, which is a good assumption given theoretical expectations and current experimental limits [2–4]. However, as discussed in Ref. [5], knowledge of F_+ also allows such D-decays to be used to study *CP*-violating observables and mixing parameters through time-dependent measurements at facilities where the mesons are produced incoherently.

The remainder of the Letter is structured as follows. Section 2 introduces the *CP*-even fraction F_+, derives the relations that are used to measure its value at the $\psi(3770)$ resonance, and reviews how knowledge of F_+ allows non-*CP* eigenstates to be cleanly employed in the measurement of γ with $B^{\mp} \to DK^{\mp}$ decays. Section 3 describes the data set and event selection.

Sections 4, 5 and 6 presents the determination of F_+ using CP tags, $D \to K^0_{\rm S,L}\pi^+\pi^-$ tags and other tags. In Sect. 7 combinations of the individual sets of results are performed for each signal mode; for $D \to \pi^+\pi^-\pi^0$ and $D \to K^+K^-\pi^0$ these combinations include the results from Ref. [1]. Section 8 gives the conclusions.

2. Measuring the CP content of a self-conjugate D-meson decay and the consequences for the γ determination with $B^\mp \to DK^\mp$

Let the amplitude of a D^0 meson decaying to a self-conjugate final state f be written as $\mathcal{A}(D^0 \to f(\mathbf{x})) \equiv a_x e^{i\theta_x}$, where $\mathbf{x}$ indicates a particular point in the decay phase space and θ_x is a CP-conserving strong phase. The amplitude is normalised such that

$$\int_{\mathbf{x}\in\mathcal{D}} |\mathcal{A}(D^0 \to f(\mathbf{x}))|^2 \,\mathrm{d}\mathbf{x} = \mathcal{B}(f), \tag{1}$$

where $\mathcal{B}(f)$ is the branching fraction of the D^0 decay and $\mathcal{D}$ indicates the entire phase space. The notation $-\mathbf{x}$ indicates the point in phase space reached by inverting the coordinates of the point at $\mathbf{x}$. The D^0 decay amplitude at $-\mathbf{x}$ is denoted $a_{-x}e^{i\theta_{-x}}$. CP violation is neglected, which implies that the $\overline{D}^0$ decay amplitude at $-\mathbf{x}$ is equal to D^0 amplitude at $\mathbf{x}$. It is useful to define the strong phase difference $\Delta\theta_x \equiv \theta_x - \theta_{-x}$.

It is possible to express the CP-even fraction in terms of the decay amplitudes introduced above. Let the CP eigenstates be $|D_{CP\pm}\rangle \equiv (|D^0\rangle \pm |\overline{D}^0\rangle)/\sqrt{2}$ and consider the decay $D^0 \to f$ in terms of these states. The total CP-even fraction of the inclusive decay is defined as

$$F_+^f \equiv \frac{\int_{\mathbf{x}\in\mathcal{D}} |\langle f(\mathbf{x})|D_{CP+}\rangle|^2 \,\mathrm{d}\mathbf{x}}{\int_{\mathbf{x}\in\mathcal{D}} |\langle f(\mathbf{x})|D_{CP+}\rangle|^2 + |\langle f(\mathbf{x})|D_{CP-}\rangle|^2 \,\mathrm{d}\mathbf{x}}, \tag{2}$$

and so

$$\begin{aligned} F_+^f &= \frac{\int_{\mathbf{x}\in\mathcal{D}} a_x^2 + a_{-x}^2 + 2a_x a_{-x}\cos\Delta\theta_x \,\mathrm{d}\mathbf{x}}{\int_{\mathbf{x}\in\mathcal{D}} 2(a_x^2 + a_{-x}^2)\,\mathrm{d}\mathbf{x}} \\ &= \frac{1}{2}\left[1 + \frac{1}{\mathcal{B}(f)}\int_{\mathbf{x}\in\mathcal{D}} a_x a_{-x}\cos\Delta\theta_x \,\mathrm{d}\mathbf{x}\right]. \end{aligned} \tag{3}$$

Note also that the following relation is always true due to the absence of *CP* violation:

$$\int_{\mathbf{x}\in\mathcal{D}} a_x a_{-x} \sin\Delta\theta_x \,\mathrm{d}\mathbf{x} = 0. \tag{4}$$

Now consider a quantum-correlated $D^0\overline{D}^0$ system produced in the decay of a $\psi(3770)$ meson. One of the D mesons in the system decays to f at the point $\mathbf{x}$, the other to g at $\mathbf{y}$, where in general the phase space of the two decays is different. The amplitude of the latter decay is denoted $b_y e^{i\phi_y}$ in analogy with the terminology used above.

The amplitude of the correlated wavefunction can be written [18]

$$\mathcal{A}(f(\mathbf{x})|g(\mathbf{y})) = \frac{1}{\sqrt{2}}\left[a_x e^{i\theta_x} b_{-y} e^{i\phi_{-y}} - a_{-x} e^{i\theta_{-x}} b_y e^{i\phi_y}\right]. \tag{5}$$

The resulting decay probability is then

$$\begin{aligned}&\mathcal{P}(f(\mathbf{x})|g(\mathbf{y})) \propto \\ &\Big[a_x^2 b_{-y}^2 + a_{-x}^2 b_y^2 - 2a_x b_{-y} a_{-x} b_y \Big(\cos\Delta\theta_x \cos\Delta\phi_y + \sin\Delta\theta_x \sin\Delta\phi_y\Big)\Big].\end{aligned} \tag{6}$$

If both D mesons decay to the same final state the probability is divided by two to avoid double counting. This formula can be used to determine the population of quantum-correlated decays either integrated over all phase space or after dividing the phase space into bins.

The number of 'double-tagged' candidates in which one D meson decays to f and the other to g, integrating over the phase space of each decay, is

$$M(f|g) = \mathcal{Z}\mathcal{B}(f)\mathcal{B}(g)\Big[1 - \Big(2F_+^f - 1\Big)\Big(2F_+^g - 1\Big)\Big], \tag{7}$$

where $\mathcal{Z}$ is a normalisation constant common to all decay modes. An important special case, considered in Sect. 4, is where the tagging-mode g is a *CP* eigenstate, and $(2F_+^g - 1)$ reduces to ± 1. Section 6 describes an analysis of classes of double-tags where this is not the case.

Alternatively, when the tagging-mode g is a multibody decay, its phase space may be divided into bins. Integrating over the phase space of f results in the following decay probability in bin i of the phase space of g:

$$\mathcal{P}(f|g_i) \propto \int_{\mathbf{y}\in\mathcal{D}_i} b_y^2 + b_{-y}^2 - \Big(2F_+^f - 1\Big) b_y b_{-y} \cos\Delta\phi_y \,\mathrm{d}\mathbf{y}, \tag{8}$$

where $\mathcal{D}_i$ indicates the phase space encompassed by bin i. In Sect. 5 this relation is exploited for the tags $D \to K^0_{\rm S,L}\pi^+\pi^-$.

To understand the relevance of the *CP*-even fraction in the measurement of the unitarity-triangle angle γ consider the decay of a B^- meson to DK^-, following which the D meson decays to a self-conjugate final state f consisting of three or more particles. The amplitude of the B^- decay is a superposition of two decay paths:

$$\mathcal{A}(B^-) = \mathcal{A}(B^- \to D^0 K^-)\mathcal{A}(D^0 \to f) + \mathcal{A}(B^- \to \overline{D}^0 K^-)\mathcal{A}(\overline{D}^0 \to f). \quad (9)$$

Following the formalism developed above, the decay amplitude of the D^0 meson at the point $\mathbf{x}$ in the phase space is denoted $a_x e^{i\theta_x}$. The decay amplitude of the B^- meson at this point in phase space is therefore

$$\mathcal{A}(B^-(\mathbf{x})) = a_x e^{i\theta_x} + r_B e^{i(\delta_B - \gamma)} a_{-x} e^{i\theta_{-x}}, \quad (10)$$

where r_B and δ_B are respectively the ratio of moduli and the strong phase difference between the suppressed and favoured B^- decays. The resulting decay probability is

$$\begin{aligned}\mathcal{P}(B^-(\mathbf{x})) &\propto a_x^2 + r_B^2 a_{-x}^2 + 2r_B a_x a_{-x}\cos\left(\delta_B - \gamma + \theta_x - \theta_{-x}\right) \\ &= a_x^2 + r_B^2 a_{-x}^2 + 2r_B a_x a_{-x}\Big[\cos(\delta_B - \gamma)\cos\Delta\theta_x - \sin(\delta_B - \gamma)\sin\Delta\theta_x\Big].\end{aligned} \quad (11)$$

The expression for B^+ decays is identical except that the sign in front of γ is flipped. The total yield of $B^\mp$ decays is determined by integrating over the entire D phase space:

$$\begin{aligned}Y^\mp &= h^\mp \int_{\mathbf{x}\in\mathcal{D}} \mathcal{P}(B^\mp(\mathbf{x}))\,{\rm d}\mathbf{x} \\ &= h^\mp\left[1 + r_B^2 + \Big(2F_+^f - 1\Big)\,2r_B\cos(\delta_B \mp \gamma)\right],\end{aligned} \quad (12)$$

where $h^\mp$ is a normalisation constant and Eqs. 3 and 4 have been employed. This expression is very similar to that derived in Ref. [7] for the case when the D meson decays to a *CP* eigenstate and is indeed identical in the event $F_+^f = 0$ or 1. Hence measurements of $Y^\mp$, and observables built from these yields [1], can be used to obtain information on the angle γ and the other parameters of the $B^\mp$ decay, provided that F_+^f is known. In Ref. [1] it is demonstrated how the effects of $D^0\overline{D}^0$ mixing, neglected in Eq. 12, may also be accommodated.

3. Data set and event selection

The data set analysed consists of e^+e^- collisions produced by the Cornell Electron Storage Ring (CESR) at $\sqrt{s} = 3.77$ GeV corresponding to an integrated luminosity of 818 pb^{-1} and collected with the CLEO-c detector. The CLEO-c detector is described in detail elsewhere [8]. Monte Carlo simulated samples of signal decays are used to estimate selection efficiencies. Possible background contributions are determined from a generic $D^0\overline{D}^0$ simulated sample corresponding to approximately fifteen times the integrated luminosity of the data set. The EVTGEN generator [9] is used to simulate the decays. The detector response is modelled using the GEANT software package [10].

Table 1 lists the D-meson final states considered in the analysis. Double-tag candidates are reconstructed in which one D meson decays into $\pi^+\pi^-\pi^+\pi^-$ and the other into a *CP* eigenstate, or where one D meson decays into $\pi^+\pi^-\pi^+\pi^-$, $\pi^+\pi^-\pi^0$ or $K^+K^-\pi^0$ and the other into one of the mixed-*CP* modes $K^0_S\pi^+\pi^-$ or $K^0_L\pi^+\pi^-$. The combinations $\pi^+\pi^-\pi^+\pi^-$ vs. $\pi^+\pi^-\pi^+\pi^-$ and $\pi^+\pi^-\pi^+\pi^-$ vs. $\pi^+\pi^-\pi^0$ are also reconstructed.

Table 1: D-meson final states reconstructed in this analysis.

Type	Final states
Mixed *CP*	$\pi^+\pi^-\pi^+\pi^-$, $\pi^+\pi^-\pi^0$, $K^+K^-\pi^0$, $K^0_{S,L}\pi^+\pi^-$
CP-even	K^+K^-, $\pi^+\pi^-$, $K^0_S\pi^0\pi^0$, $K^0_L\pi^0$, $K^0_L\omega$
CP-odd	$K^0_S\pi^0$, $K^0_S\omega$, $K^0_S\eta$, $K^0_S\eta'$

The unstable final state particles are reconstructed in the following decay modes: $\pi^0 \to \gamma\gamma$, $K^0_S \to \pi^+\pi^-$, $\omega \to \pi^+\pi^-\pi^0$, $\eta \to \gamma\gamma$, $\eta \to \pi^+\pi^-\pi^0$ and $\eta' \to \eta(\gamma\gamma)\pi^+\pi^-$. The π^0, K^0_S, ω, η and η' reconstruction procedure is identical to that used in Ref. [12].

Final states that do not contain a K^0_L are fully reconstructed via the beam-constrained candidate mass, $m_{\rm bc} \equiv \sqrt{s/4c^4 - \mathbf{p}_D^2/c^2}$, where $\mathbf{p}_D$ is the D-candidate momentum, and $\Delta E \equiv E_D - \sqrt{s}/2$, where E_D is the D-candidate energy. The $m_{\rm bc}$ and ΔE distributions of correctly reconstructed D-meson candidates will peak at the nominal D^0 mass and zero, respectively. Neither ΔE nor $m_{\rm bc}$ distributions exhibit any peaking structure for combinatoric background. The double-tag yield is determined from counting events in

signal and sideband regions of $m_{\rm bc}$ after placing requirements on ΔE [1, 11–13]. The selection criteria of candidates involving the modes $D \to K^+K^-$ and $D \to \pi^+\pi^-$ do not include the cosmic ray muon and radiative Bhabha vetoes that are described in Ref. [1]. This is because these sources of background do not contaminate the double-tag sample, and the vetoes are found to perturb the selection efficiency of the other D meson in the event. When selecting $D \to K^0_{\rm S}\pi^+\pi^-$ candidates it is demanded that the $K^0_{\rm S}$ decay products form a vertex that is significantly displaced from the e^+e^- collision point; in contrast, for $D \to \pi^+\pi^-\pi^+\pi^-$ and $D \to \pi^+\pi^-\pi^0$ candidates the $\pi^+\pi^-$ vertex must be consistent with originating from the collision point in order to suppress contamination from $D \to K^0_{\rm S}\pi^+\pi^-$ and $D \to K^0_{\rm S}\pi^0$ decays, respectively.

The double-tag yield determination procedure is identical to that presented in Refs. [11, 12] except for the selections where the signal decay is $\pi^+\pi^-\pi^+\pi^-$ and the tag decay is K^+K^-, $\pi^+\pi^-$, $\pi^+\pi^-\pi^0$ or $\pi^+\pi^-\pi^+\pi^-$, which are all dominated by a background from continuum production of light quark-antiquark pairs. For these modes an unbinned maximum likelihood fit is performed to the distribution of the average $m_{\rm bc}$ of the two D-meson candidates. The background is modelled with an ARGUS function [14] and the signal is modelled with the sum of two Crystal Ball functions [15] with power-law tails on opposite sides. The parameters of the Crystal Ball functions are fixed from fits to large samples of simulated data.

Figures 1 (a) and (b) show the average $m_{\rm bc}$ distributions for CP-tagged $D \to \pi^+\pi^-\pi^+\pi^-$ candidates, summed over all CP-even and CP-odd tags, respectively, where the CP-tag final state does not contain a $K^0_{\rm L}$ meson. Figure 2 shows the average $m_{\rm bc}$ distributions for $D \to \pi^+\pi^-\pi^+\pi^-$, $D \to \pi^+\pi^-\pi^0$ and $D \to K^+K^-\pi^0$ candidates tagged with $D \to K^0_{\rm S}\pi^+\pi^-$ decays, while Fig. 3 shows the Dalitz-plot distributions of the tag decay for these three signal modes.

Many $K^0_{\rm L}$ mesons do not deposit any reconstructible signal in the detector. However, double-tag candidates can be fully reconstructed using a missing-mass squared ($m^2_{\rm miss}$) technique [16] for tags containing a single $K^0_{\rm L}$ meson. Yields are determined from the signal and sideband regions of the $m^2_{\rm miss}$ distribution. Figure 1 (c) shows the $m^2_{\rm miss}$ distributions for $D \to \pi^+\pi^-\pi^+\pi^-$ candidates tagged with either a $K^0_{\rm L}\pi^0$ or $K^0_{\rm L}\omega$ decay. Figure 4 shows the $m^2_{\rm miss}$ distributions for $D \to \pi^+\pi^-\pi^+\pi^-$, $D \to \pi^+\pi^-\pi^0$ and $D \to K^+K^-\pi^0$ candidates tagged with $D \to K^0_{\rm L}\pi^+\pi^-$ decays, and Fig. 5 shows the corresponding tag-side Dalitz-plot distributions.

In events where more than one pair of decays is reconstructed an algo-

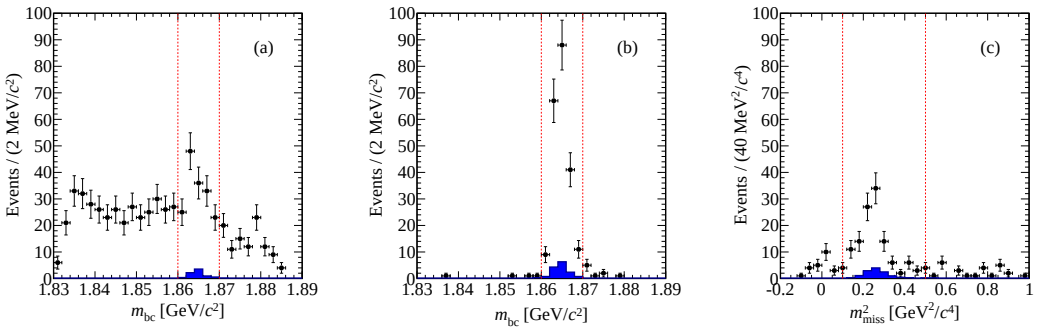

Figure 1: Distributions of $D \to \pi^+\pi^-\pi^+\pi^-$ candidates tagged by *CP*-eigenstates. Sub-figures (a) and (b) show average $m_{\rm bc}$ distributions for *CP*-even tags and *CP*-odd tags not involving $K^0_{\rm L}$ mesons, respectively. Sub-figure (c) shows the $m^2_{\rm miss}$ distribution for candidates tagged by *CP* eigenstates that contain a $K^0_{\rm L}$ meson. The shaded histogram is the estimated peaking background and the vertical dotted lines indicate the signal region.

rithm is applied to select a single double-tag candidate based on the information provided by the $m_{\rm bc}$ and ΔE variables. The precise choice of metric varies depending on the category of double tag and is optimised through simulation studies.

The peaking background estimates are determined from the generic Monte Carlo sample of $D\overline{D}$ events. For double tags involving a *CP* mode without a $K^0_{\rm L}$ meson the peaking backgrounds are found to be 5-10%. The peaking backgrounds for final states with a $K^0_{\rm L}$ are generally larger; for $K^0_{\rm L}\pi^0$ and $K^0_{\rm L}\omega$ they are 15–20% of the signal yield, whereas for $K^0_{\rm L}\pi^+\pi^-$ they are $\sim 10\%$ of the signal yield. The dominant source of peaking background in each case is the equivalent decay containing a $K^0_{\rm S}$ instead of a $K^0_{\rm L}$ meson. The contamination from specific modes in the other categories of double tags is typically 10% or less and is discussed in more detail in Sects. 5 and 6. The statistical uncertainties on these background estimates arising from the finite size of the simulated samples is included in the total statistical uncertainties on the signal yields.

The measured double-tag event yields after background subtraction are given in Table 2.

Knowledge of the single-tag yields of the *CP*-eigenstate modes is required for normalisation purposes. Since the single-tag reconstruction criteria applied are identical to those employed in Ref. [1], all information on these yields is taken from the earlier publication. It is also necessary to know the

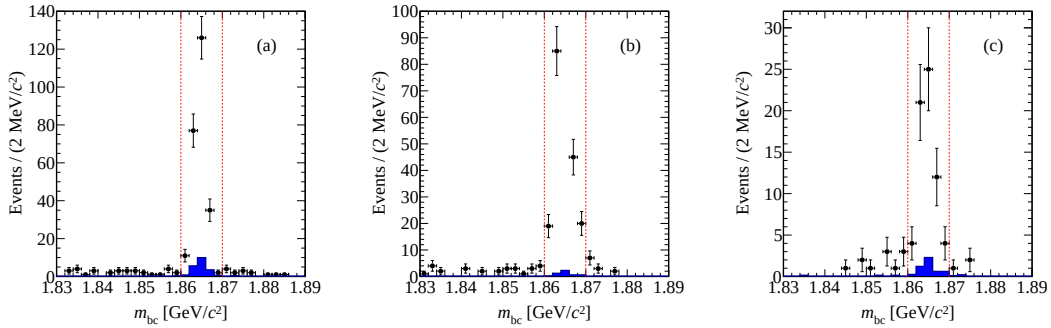

Figure 2: Average $m_{\rm bc}$ distributions for (a) $D \to \pi^+\pi^-\pi^+\pi^-$, (b) $D \to \pi^+\pi^-\pi^0$ and (c) $D \to K^+K^-\pi^0$ candidates tagged by a $D \to K^0_S\pi^+\pi^-$ decay. The shaded histogram is the estimated peaking background and the vertical dotted lines indicate the signal region.

single-tag yield for the decay $D \to \pi^+\pi^-\pi^0$. A fit to the $m_{\rm bc}$ distribution returns a result of 29998 ± 320 signal candidates after the subtraction of small peaking-background contributions.

4. Analysis with the *CP* tags

The yields of the single and double tags containing a *CP* eigenstate are used as inputs to determine the CP-even fraction, $F_+^{4\pi}$. Following on from Eq. 7, the expected number of observed events, M, where one D meson decays to the $\pi^+\pi^-\pi^+\pi^-$ final state, and the other decays to a X, a *CP* eigenstate with eigenvalue η_{CP}, is given by

$$M(4\pi|X) = 2N_{D\bar{D}}\,\mathcal{B}(4\pi)\mathcal{B}(X)\varepsilon(4\pi|X)\left[1 - \eta_{CP}\left(2F_+^{4\pi} - 1\right)\right], \qquad (13)$$

where $N_{D\bar{D}}$ is the number of $D\overline{D}$ pairs, $\mathcal{B}(4\pi)$ and $\mathcal{B}(X)$ are the branching fractions for the two reconstructed final states and $\varepsilon(4\pi|X)$ is the efficiency of reconstructing such a double tag. The double tag yield is denoted by M^- (M^+) for *CP*-even (*CP*-odd) tags. Experimentally it is advantageous to eliminate dependence on knowledge of $N_{D\bar{D}}$, the branching fractions and the reconstruction efficiency, which can be achieved by normalising by the single-tag yields. The yields of single tags, S^+ (S^-) decaying to a *CP*-odd (*CP*-even) eigenstate X, is given by

$$S(X) = 2N_{D\bar{D}}\,\mathcal{B}(X)\varepsilon(X), \qquad (14)$$

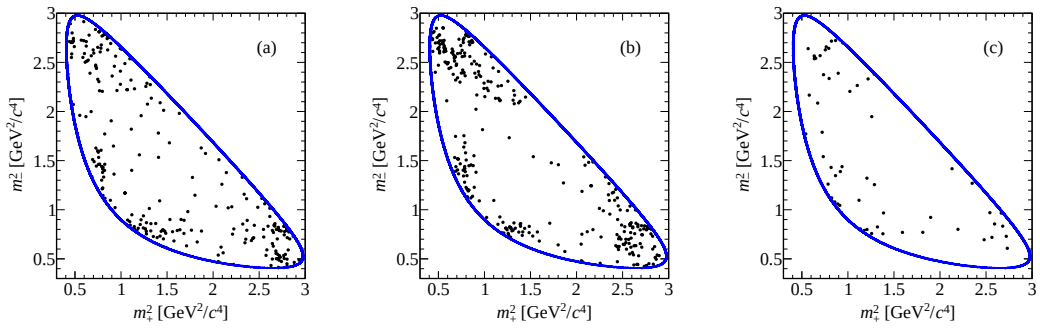

Figure 3: Dalitz-plot distributions for $D \to K^0_S\pi^+\pi^-$ reconstructed against (a) $D \to \pi^+\pi^-\pi^+\pi^-$, (b) $D \to \pi^+\pi^-\pi^0$ and (c) $D \to K^+K^-\pi^0$. The axis labels $m^2_\pm$ are the invariant-mass squared of the $\pi^\pm K^0_S$ pair.

where $\varepsilon(X)$ is the reconstruction efficiency of the single tag. The small effects of $D^0\overline{D}^0$ mixing are eliminated from the measurement by correcting the measured single tags yields $S^\pm_{\rm meas}$ such that $S^\pm = S^\pm_{\rm meas}/(1 - \eta_{CP}y_D)$ where $y_D = (0.62 \pm 0.08)\%$ is the well-known D-mixing parameter [17]. A further correction is applied in the case of the tags K^+K^- and $\pi^+\pi^-$ because of the differing selection requirements for the single and double-tag case, as described in Sect. 3. This correction factor is determined by taking the ratio of selection efficiency of the single tag from simulation with the two differing selections. It is determined to be 1.15±0.05 and 1.10±0.05 for the $D \to K^+K^-$ and $D \to \pi^+\pi^-$ modes, respectively. The uncertainty is based on the muon identification uncertainty in the simulation. **more thought needed about this last sentence**

Assuming that the reconstruction efficiencies of each D meson are independent, then the ratio of the double-tagged and single-tagged yields are independent of the branching fraction and reconstruction efficiency of the CP tag and $N_{D\overline{D}}$. This ratio is defined as $N^+ \equiv M^+/S^+$, with an analogous expression for N^-. The CP-even fraction $F^{4\pi}_+$ is then given by

$$F^{4\pi}_+ = \frac{N^+}{N^+ + N^-}. \tag{15}$$

The measured values for N^+ and N^- for each CP tag are displayed in Fig. 6. It can be seen that there is consistency between the individual tags for each measurement and that N^+ is significantly larger than N^-, indicating that the $\pi^+\pi^-\pi^+\pi^-$ final state is predominantly CP even.

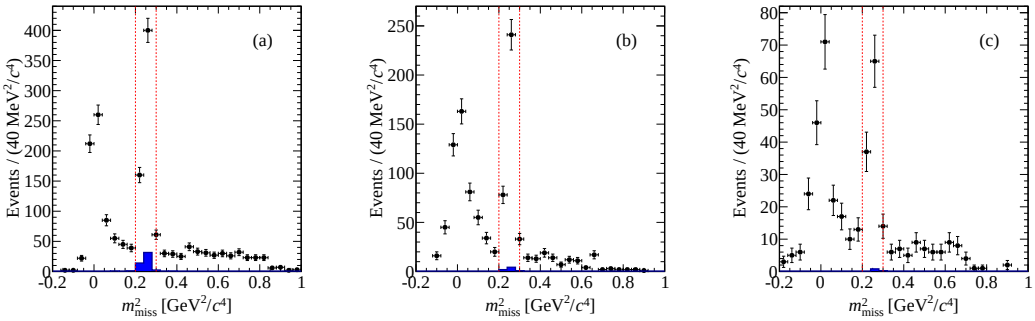

Figure 4: $m^2_{\rm miss}$ distributions for (a) $D \to \pi^+\pi^-\pi^+\pi^-$, (b) $D \to \pi^+\pi^-\pi^0$ and (c) $D \to K^+K^-\pi^0$ candidates tagged by a $D \to K^0_{\rm L}\pi^+\pi^-$ decay. The shaded histogram is the estimated peaking background and the vertical dotted lines indicate the signal region.

There is an uncertainty in the single-tag yields of those tags not involving a $K^0_{\rm L}$ meson due to the fit function used to model the distribution in the $m_{\rm bc}$ variable. The uncertainty on this shape depends on the presence of neutral particles and their momentum spectrum. The decays to $K^0_{\rm S}\pi^0$ and $K^0_{\rm S}\eta(\gamma\gamma)$ contain relatively hard neutrals and have a 2.5% uncertainty applied to the single tag yield. All other *CP* tags involving a $K^0_{\rm S}$ meson contain a relatively soft neutral particle and are assigned a 5% uncertainty on their yield. Uncertainties of 2% are applied to the K^+K^- and $\pi^+\pi^-$ single tags for uncertainties in the fit model, with a further 5% applied to take into account the selection correction factors. These assignments also adequately cover those uncertainties related to the assumption of the double-tag efficiency factorising into the product of the two single-tag efficiencies. A further small systematic uncertainty is assigned to account for the limited knowledge of the mixing parameter y_D. No uncertainty is assigned for the imperfect knowledge of the branching fractions of the modes that contribute to the peaking backgrounds, as it would be small compared with the corresponding statistical uncertainty on this source of contamination.

For the case of the two *CP* tags involving a $K^0_{\rm L}$ meson a different treatment is required, since it is not possible to measure the single-tag yield directly for these modes. The effective single-tag yield is determined from Eq. 14, where the effective single-tag efficiency $\varepsilon(K^0_{\rm L}X)$ is determined from the ratio of $\varepsilon(4\pi|K^0_{\rm L}X)/\varepsilon(4\pi)$. The leading systematic uncertainties for these effective single-tag yields come from the knowledge of the branching fractions and the

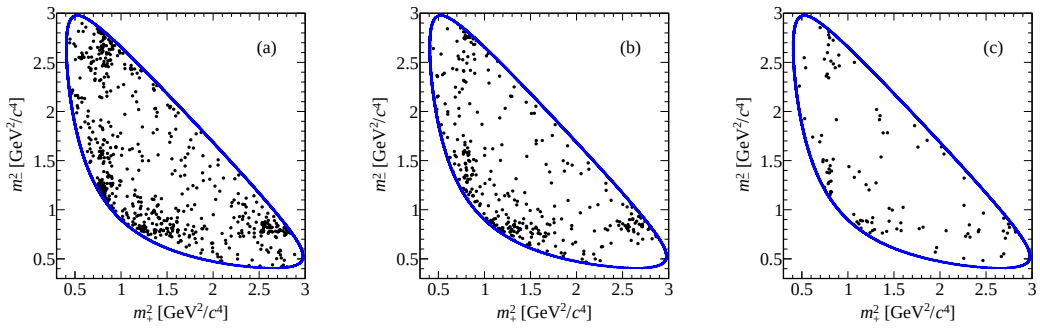

Figure 5: Dalitz-plot distributions for $D \to K^0_L\pi^+\pi^-$ reconstructed against (a) $D \to \pi^+\pi^-\pi^+\pi^-$, (b) $D \to \pi^+\pi^-\pi^0$ and (c) $D \to K^+K^-\pi^0$. The axis labels $m^2_\pm$ are the invariant-mass squared of the $\pi^\pm K^0_L$ pair.

value used for the effective single-tag efficiency. The uncertainty on $\varepsilon(K^0_L X)$ is taken as an absolute 6% due to the non-factorisation effects observed when comparing the value obtained when using different double tags. In the case of $K^0_L\omega$ the branching fraction is unmeasured and so the branching fraction for $D^0 \to K^0_S\omega$ is used with an additional uncertainty of 20% on the central value. Additional smaller uncertainties on these effective single-tag yields arise from the knowledge of $N_{D\overline{D}}$ and the size of the simulation samples used to determine $\varepsilon(K^0_L X)$. The effective single-tag yields are determined to be 21726 ± 3497 and 9124 ± 4105 for $K^0_L\pi^0$ and $K^0_L\omega$, respectively, and are consistent with those used in Ref. [1]. These systematic uncertainties are significant for both tags, and dominant for $K^0_L\omega$, as is evident from Fig. 6.

If the acceptance across the phase space of the $D \to \pi^+\pi^-\pi^+\pi^-$ decay is not uniform it has the potential to bias the measurement of $F^{4\pi}_+$ with respect to the true value. Using simulated data the selection efficiency of individual pions in $D \to \pi^+\pi^-\pi^+\pi^-$ decays is determined in bins of momentum and polar angle with respect to the beam direction. The candidates in data are then weighted by the normalised efficiency, according to which bin each pion lies in. Each pion is treated independently and an overall weight, typically lying within 5–10% of unity, is found by multiplying together the individual weights. The scaled signal yields are used to re-determine $F^{4\pi}_+$ and the difference between this and the nominal value is found to be 0.008, which is taken as the systematic uncertainty due to non-uniform acceptance.

Using the *CP* tags only, and accounting for the correlations between the

Table 2: Double-tagged signal yields after background subtraction. Information on the entries marked '†', not studied in the current analysis, can be found in Ref. [1].

	$\pi^+\pi^-\pi^+\pi^-$	$\pi^+\pi^-\pi^0$	$K^+K^-\pi^0$
K^+K^-	19.4 ± 6.3	†	†
$\pi^+\pi^-$	3.3 ± 8.2	†	†
$K^0_S\pi^0\pi^0$	18.6 ± 5.1	†	†
$K^0_L\pi^0$	49.2 ± 10.9	†	†
$K^0_L\omega$	22.0 ± 6.5	†	†
$K^0_S\pi^0$	112.8 ± 11.0	†	†
$K^0_S\omega$	41.0 ± 6.7	†	†
$K^0_S\eta(\gamma\gamma)$	18.8 ± 4.5	†	†
$K^0_S\eta(\pi^+\pi^-\pi^0)$	3.1 ± 2.7	†	†
$K^0_S\eta'$	9.3 ± 3.2	†	†
$K^0_S\pi^+\pi^-$	217.9 ± 16.8	289.2 ± 17.6	52.5 ± 7.8
$K^0_L\pi^+\pi^-$	485.0 ± 26.3	291.1 ± 19.2	78.1 ± 11.1
$\pi^+\pi^-\pi^+\pi^-$	41.0 ± 16.3	75.5 ± 15.7	—

systematic uncertainties, yields $F_+^{4\pi} = 0.754 \pm 0.031 \pm 0.021$, where the first uncertainty is statistical and the second systematic.

5. Analysis with the $D \to K^0_{S,L}\pi^+\pi^-$ tags

For each of the signal samples that are tagged by $D \to K^0_S\pi^+\pi^-$ or $D \to K^0_L\pi^+\pi^-$ decays the Dalitz plot of the tag mode is divided into eight pairs of symmetric bins by the line $m^2_+ = m^2_-$, where $m^2_\pm$ is the invariant-mass squared of the $\pi^\pm K^0_{S,L}$ pair. The bins lying on one side of this line ($m^2_+ > m^2_-$) are labelled $-1 \to -8$, and those on the other side $1 \to 8$. The binning definition follows the 'Equal $\Delta\delta_D$ BABAR 2008' scheme of Ref. [18], in which the boundaries are chosen according to the strong-phase prediction of a model developed by the BaBar collaboration [19]. The expected distribution of entries is symmetric and so the analysis considers the absolute bin number $|i|$, which contains the contents of the pair of bins $-i$ and i.

Following Eq. 8, the expected population of bin $|i|$ for signal decays with $K^0_S\pi^+\pi^-$ tags is

$$M_{|i|} = h\left[K_i + K_{-i} - \Big(2F_+ - 1\Big)2c_i\sqrt{K_iK_{-i}}\right], \qquad (16)$$

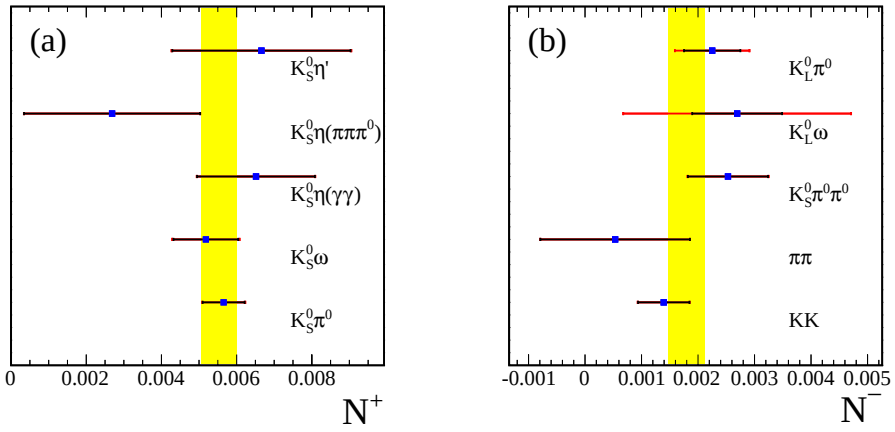

Figure 6: $D \to \pi^+\pi^-\pi^+\pi^-$ results for (a) N^+ and (b) N^-. In each plot the vertical yellow band indicates the value obtained from the combination of all tags. The black portion of the uncertainty represents the statistical uncertainty only while the red represents the total.

where h is a normalisation factor specific to the signal category, K_i is the flavour-tagged fraction, being the proportion of $K^0_S\pi^+\pi^-$ decays to fall in bin i in the case that the mother particle is known to be a D^0 meson, and c_i is the cosine of the strong-phase difference between D^0 and $\bar{D}^0$ decays averaged in bin i and weighted by the absolute decay rate (a precise definition may be found in Ref. [6]). The only difference between the form of this expression and the case when the signal decays into a pure CP-even eigenstate [6] is the prefactor of $(2F_+ - 1)$ in the final term.

Similarly, when the tagging meson decays to $K^0_L\pi^+\pi^-$ then the number of double-tag decays produced in bin $|i|$ is

$$M'_{|i|} = h' \left[K'_i + K'_{-i} + \Big(2F_+ - 1\Big) 2c'_i \sqrt{K'_i K'_{-i}} \right], \tag{17}$$

where the primed quantities are now specific to this case. The flipped sign in front of the final term reflects the fact that the K^0_L meson is almost entirely a CP-odd eigenstate.

The values of c_i and c'_i within these bins have been measured by the CLEO collaboration [18]. The values of the K_i parameters are taken from an analysis of the predictions of various B-factory models [19–22] presented in Ref. [13], and those of the K'_i parameters from measurements performed

with CLEO-c data [23].

The double-tagged samples are analysed to determine the background-subtracted signal yield in each Dalitz bin. The distribution of background between the different bins is assigned according to its category. Flat background is assumed to contribute proportionally to the bin area. Peaking backgrounds that occur on the signal side affect the distribution of tag decays in $K^0_{S,L}\pi^+\pi^-$ phase space according to their nature. For example, in the case of $D \to K^0_S\pi^0$ decays that are wrongly reconstructed as $D \to \pi^+\pi^-\pi^0$ the tag decay will be in a *CP*-even state and distributed accordingly. Similarly, the distribution of $K^0_S(\pi^0\pi^0)\pi^+\pi^-$ decays that are misreconstructed as $K^0_L\pi^+\pi^-$ tags is well understood and modelled appropriately. The distribution of the residual $K^0_S\pi^+\pi^-$ vs. $K^0_S\pi^+\pi^-$ events that contaminate the $\pi^+\pi^-\pi^+\pi^-$ vs. $K^0_S\pi^+\pi^-$ selection is determined from data by inverting the K^0_S veto on the signal decay.

It is also necessary to account for relative bin-to-bin efficiency variations in the background-subtracted signal yields. The correction factors are determined from simulation and typically differ $\sim 5\%$ from unity. The signal yields in each bin after background subtraction and relative efficiency correction are shown in Table 3 for $K^0_S\pi^+\pi^-$ tags and in Table 4 for $K^0_L\pi^+\pi^-$ tags.

Table 3: Double-tagged signal yields vs. $K^0_S\pi^+\pi^-$ after background subtraction in absolute bin numbers of the $D \to K^0_S\pi^+\pi^-$ Dalitz plot. The yields are corrected for relative bin-to-bin efficiency variations.

$\lvert i\rvert$	$\pi^+\pi^-\pi^+\pi^-$	$\pi^+\pi^-\pi^0$	$K^+K^-\pi^0$
1	30.8 ± 7.0	29.9 ± 6.3	12.6 ± 4.1
2	19.8 ± 5.3	19.1 ± 4.8	4.6 ± 2.6
3	16.4 ± 4.5	27.2 ± 5.2	6.9 ± 2.5
4	10.1 ± 3.4	18.5 ± 4.4	1.6 ± 1.5
5	55.1 ± 8.1	96.9 ± 10.0	8.4 ± 3.1
6	21.1 ± 5.1	31.2 ± 5.8	4.4 ± 2.4
7	27.7 ± 6.0	34.6 ± 6.3	7.7 ± 2.8
8	36.9 ± 6.8	31.8 ± 6.0	6.2 ± 2.5

A log-likelihood fit is performed to the efficiency-corrected signal yields of each sample, assuming the expected distributions given by Eqs. 16 and 17.

Table 4: Double-tagged signal yields vs. $K^0_L\pi^+\pi^-$ after background subtraction in absolute bin numbers of the $D^0 \to K^0_L\pi^+\pi^-$ Dalitz plot. The yields are corrected for relative bin-to-bin efficiency variations.

$\lvert i\rvert$	$\pi^+\pi^-\pi^+\pi^-$	$\pi^+\pi^-\pi^0$	$K^+K^-\pi^0$
1	134.1 ± 13.9	89.2 ± 11.1	17.3 ± 6.1
2	59.2 ± 8.9	32.9 ± 6.9	8.8 ± 4.0
3	55.4 ± 8.7	31.0 ± 6.3	4.1 ± 3.1
4	20.3 ± 5.8	7.0 ± 3.7	0.1 ± 1.9
5	46.0 ± 8.7	6.7 ± 4.8	2.1 ± 3.1
6	24.6 ± 6.2	14.7 ± 5.0	10.0 ± 3.7
7	61.2 ± 9.0	46.7 ± 7.8	17.6 ± 4.7
8	84.1 ± 10.8	62.9 ± 8.9	18.1 ± 5.1

The fit parameters are the *CP*-even fraction and the overall normalisation. The values of K_i, K'_i, c_i and c'_i are also fitted, but with their measurement uncertainties and correlations imposed as a Gaussian constraint. Separate fits are performed for the $D \to K^0_S\pi^+\pi^-$ tags, the $D \to K^0_L\pi^+\pi^-$ tags, and for both samples combined. Fits to large ensembles of simulated experiments demonstrate that the returned uncertainties are reliable and that there is no significant bias in the procedure. All data fits are found to be of good quality. The results are plotted in Fig. 7 for the $D \to K^0_S\pi^+\pi^-$ tags and in Fig. 8 for the $D \to K^0_L\pi^+\pi^-$ tags. The numerical results for the *CP*-even fraction are given in Table 5 for $D \to \pi^+\pi^-\pi^+\pi^-$ and in Table 6 for $D \to \pi^+\pi^-\pi^0$ and $D \to K^+K^-\pi^0$.

Table 5: The $F^{4\pi}_+$ fit results for the $D \to K^0\pi^+\pi^-$ tags, where the first uncertainty is statistical and the second systematic. The row $K^0_{S,L}\pi^+\pi^-$ indicates the configuration where the *CP*-even fraction is a common fit parameter shared between the $D \to K^0_S\pi^+\pi^-$ and $D \to K^0_L\pi^+\pi^-$ samples. The goodness of fit is also given.

Tag	$F^{4\pi}_+$	χ^2/n.d.f.
$K^0_S\pi^+\pi^-$	0.828 ± 0.074 ± 0.014	3.8/6
$K^0_L\pi^+\pi^-$	0.670 ± 0.057 ± 0.039	4.3/6
$K^0_{S,L}\pi^+\pi^-$	0.737 ± 0.049 ± 0.024	5.2/13

Table 6: The $F_+^{\pi\pi\pi^0}$ and $F_+^{KK\pi^0}$ fit results for the $D \to K^0\pi^+\pi^-$ tags, where the first uncertainty is statistical and the second systematic. The row $K^0_{S,L}\pi^+\pi^-$ indicates the configuration where the *CP*-even fraction is a common fit parameter shared between the $D \to K^0_S\pi^+\pi^-$ and $D \to K^0_L\pi^+\pi^-$ samples. The goodness of fit is also given.

Tag	$F_+^{\pi\pi\pi^0}$	χ^2/n.d.f.	$F_+^{KK\pi^0}$	χ^2/n.d.f.
$K^0_S\pi^+\pi^-$	$1.034 \pm 0.054 \pm 0.023$	3.0/6	$0.573 \pm 0.152 \pm 0.046$	1.5/6
$K^0_L\pi^+\pi^-$	$0.971 \pm 0.075 \pm 0.033$	1.1/6	$0.916 \pm 0.181 \pm 0.066$	7.8/6
$K^0_{S,L}\pi^+\pi^-$	$1.014 \pm 0.045 \pm 0.022$	3.1/13	$0.734 \pm 0.106 \pm 0.054$	2.6/13

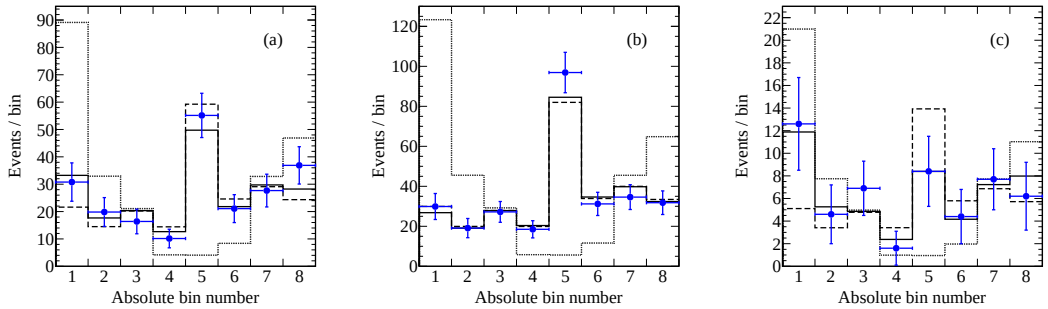

Figure 7: Data (points) and fit results (solid line) in absolute bin numbers for $K^0_S\pi^+\pi^-$ tags vs. (a) $D \to \pi^+\pi^-\pi^+\pi^-$, (b) $D \to \pi^+\pi^-\pi^0$ and (c) $D \to K^+K^-\pi^0$. Also shown in each case is the expectation if $F_+ = 0$ (dotted line) or $F_+ = 1$ (dashed line).

Systematic uncertainties are assigned to account for alternative methods of distributing the background between the Dalitz bins. In the case of the peaking background the results from the analysis of a Monte Carlo sample are used, and for the continuum and combinatoric components the distribution is switched to that found in the sidebands of the signal distributions. The uncertainty associated with the measurement errors on K_i, K'_i, c_i and c'_i is estimated by re-running the fit with these quantities set as fixed parameters and subtracting in quadrature the new fit uncertainty from that obtained with the original procedure. This component is found to be 0.013 for $D \to \pi^+\pi^-\pi^+\pi^-$, 0.010 for $D \to \pi^+\pi^-\pi^0$ and 0.025 for $D \to K^+K^-\pi^0$, and is accounted as a systematic uncertainty in the final results. A small uncertainty is assigned arising from the choice of algorithm used to select between reconstructed decays in events with multiple candidates. Finally, an

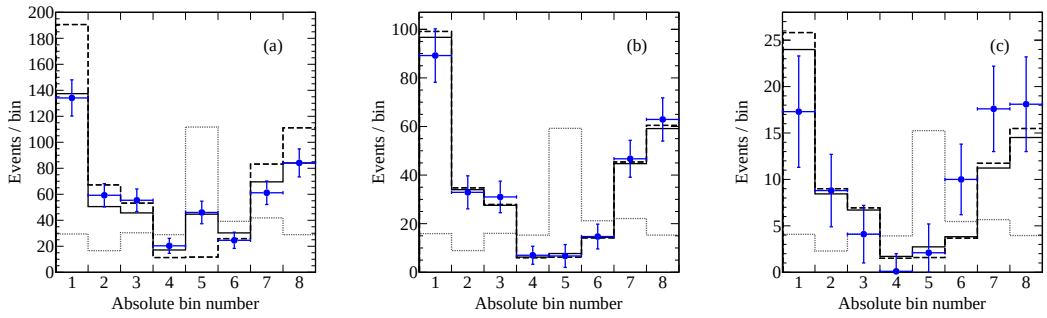

Figure 8: Data (points) and fit results (solid line) in absolute bin numbers for $K^0_L\pi^+\pi^-$ tags vs. (a) $D \to \pi^+\pi^-\pi^+\pi^-$, (b) $D \to \pi^+\pi^-\pi^0$ and (c) $D \to K^+K^-\pi^0$. Also shown in each case is the expectation if $F_+ = 0$ (dotted line) or $F_+ = 1$ (dashed line).

uncertainty is evaluated to account for non-uniformities in acceptance across phase space. For $D \to \pi^+\pi^-\pi^+\pi^-$ this contribution is calculated with the same procedure as in Sect. 4, and found to be 0.002 for the joint $K^0_{S,L}\pi^+\pi^-$ fit. For $D \to \pi^+\pi^-\pi^0$ and $D \to K^+K^-\pi^0$ the acceptance uncertainties are taken to be 0.001 and 0.010, respectively, as determined in Ref. [1]. The total systematic uncertainties are given in Tables 5 and 6 and are in all cases significantly smaller than the corresponding statistical uncertainties.

6. Other tags

The double-tagged yield of $\pi^+\pi^-\pi^+\pi^-$ vs. $\pi^+\pi^-\pi^0$ can be used to determine $F_+^{4\pi}$, benefitting from the well-measured value of $F_+^{\pi\pi\pi^0}$. The ratio of double-tag and $D \to \pi^+\pi^-\pi^0$ single-tag yields is defined as $N^{\pi\pi\pi^0} \equiv M(4\pi|\pi\pi\pi^0)/S(\pi\pi\pi^0)$, where a very small correction is applied to the measured single-tag yield to account for mixing effects. Following from Eq. 7, the ratio $N^{\pi\pi\pi^0}/N^+$ removes dependence on knowledge of the signal branching fraction and reconstruction efficiency and is given by

$$\frac{N^{\pi\pi\pi^0}}{N^+} = \frac{\left[1 - \left(F_+^{4\pi} - 1\right)\left(2F_+^{\pi\pi\pi^0} - 1\right)\right]}{2\left(1 - F_+^{\pi\pi\pi^0}\right)}, \tag{18}$$

which can be rearranged to yield

$$F_+^{4\pi} = \frac{N^+ F_+^{\pi\pi\pi^0}}{N^{\pi\pi\pi^0} - N^+ + 2N^+ F_+^{\pi\pi\pi^0}}. \tag{19}$$

The choice of N^+ in the denominator of Eq. 18 is preferred to N^- as it is measured with better relative precision.

Taking as input the yields given in Sect. 3, the value of N^+ reported in Sect. 4 and the final result for $F_+^{\pi\pi\pi^0}$ presented in Sect. 7 implies $F_+^{4\pi} = 0.695 \pm 0.050 \pm 0.021$, where the uncertainties are statistical and systematic, respectively. There are several contributions to the systematic component. An uncertainty of 5% is assigned to the $D \to \pi\pi\pi^0$ single-tag yield to account for imperfections in the fit parameterisation, and also accounts for small violations of the efficiency-factorisation ansatz assumed in Eq. 18 as assessed from simulation studies. The double-tag yield of $\pi^+\pi^-\pi^+\pi^-$ vs. $\pi^+\pi^-\pi^0$ has a peaking background from $\pi^+\pi^-\pi^+\pi^-$ vs. $K^0_S\pi^0$ decays in which the K^0_S candidate is misidentified as two charged prompt pions. The value of this contamination as measured in the the Monte Carlo is an underestimate, since the simulation does not include the enhancement driven by the quantum correlations and the dominant *CP*-even content of the $D \to \pi^+\pi^-\pi^+\pi^-$ decay. Hence the raw result is scaled assuming a central value of $F_+^{4\pi}$ as given by the analysis of the *CP* tags, and a systematic uncertainty of 0.004 is determined from varying this input by $\pm 5\%$. The effect of non-uniform acceptance is evaluated with the same procedure described in Sect. 4 and leads to an uncertainty on $F_+^{4\pi}$ of 0.016. Further small uncertainties arise from the precision in the measurement of $F_+^{\pi\pi\pi^0}$, the knowledge of the mixing parameter y_D, and the exact treatment of events containing multiple candidates.

The self-tagged yield of $\pi^+\pi^-\pi^+\pi^-$ vs. $\pi^+\pi^-\pi^+\pi^-$ also carries information on the value of $F_+^{4\pi}$. This sample is however only used for a consistency check, as there are large backgrounds from both the continuum and from misidentification of $D \to K^0_S\pi\pi$ decays that are a potential source of significant systematic bias. Furthermore, the predicted yield and measurement uncertainty means that the result from analysis of these double tags would have low weight in the combined measurement of $F_+^{4\pi}$. Using Eq. 7 the number of observed self tagged events is given by

$$M(4\pi|4\pi) = 4\mathcal{R}F_+^{4\pi}\Big(1 - F_+^{4\pi}\Big), \tag{20}$$

where $\mathcal{R} = N_{D\bar{D}}(BR_{4\pi})^2\varepsilon(4\pi|4\pi)$. The predicted double-tagged yield using the value of $F_+^{4\pi}$ obtained from the *CP* tags is 17$\pm$2, which is consistent with the measured yield reported in Table 2.

7. Combination of results

The results for $F_+^{4\pi}$ from the *CP* tags, the $K^0_{\rm S,L}\pi^+\pi^-$ tags and the $\pi^+\pi^-\pi^0$ tag are summarised in Table 7. They are compatible and are therefore combined, taking account of correlated uncertainties. Correlations arise from the non-flat Dalitz plot acceptance between all three measurements and the use of N^+ as an input to both the *CP* tags and $\pi^+\pi^-\pi^0$ tag measurements. There is a further small correlation between the results obtained with the *CP* and $\pi^+\pi^-\pi^0$ tags, associated with the uncertainty on the value of the mixing parameter y_D. The final result is $F_+^{4\pi} = 0.737 \pm 0.028$.

Table 7: Results for $F_+^{4\pi}$ for each tag category, and combined. When two uncertainties are shown, the first is statistical and the second systematic. For the combined result the total uncertainty is given.

Tag	$F_+^{4\pi}$
CP eigenstates	$0.754 \pm 0.031 \pm 0.021$
$K^0_{\rm S,L}\pi^+\pi^-$	$0.737 \pm 0.049 \pm 0.024$
$\pi^+\pi^-\pi^0$	$0.695 \pm 0.050 \pm 0.021$
Combined	0.737 ± 0.028

Table 8 summarises the results on $F_+^{\pi\pi\pi^0}$ and $F_+^{KK\pi^0}$ obtained with the $K^0_{\rm S,L}\pi^+\pi^-$ tags, together with those determined from *CP* tags [1]. The $K^0_{\rm S,L}\pi^+\pi^-$ measurements confirm the results of the earlier analysis. A combination is performed, accounting for the sole source of correlated uncertainties, which is that arising from the non-uniform acceptance over the Dalitz plots. Results of $F_+^{\pi\pi\pi^0} = 0.973 \pm 0.017$ and $F_+^{KK\pi^0} = 0.732 \pm 0.055$ are obtained. The $K^0_{\rm S,L}\pi^+\pi^-$ tags improve the relative precision on $F_+^{\pi\pi\pi^0}$ by 6% and on $F_+^{KK\pi^0}$ by 10%.

8. Conclusions

A first measurement has been made of the *CP*-even fraction of the decay $D \to \pi^+\pi^-\pi^+\pi^-$, exploiting quantum-correlated double-tags involving *CP*-eigenstates, a binned Dalitz-plot analysis of the modes $D \to K^0_{\rm S,L}\pi^+\pi^-$, and $D \to \pi^+\pi^-\pi^0$ decays. The result, $F_+^{4\pi} = 0.737 \pm 0.028$, when considered alongside the relatively high branching fraction, indicates that this channel is a valuable addition to the suite of D-decays that can be harnessed for the

Table 8: Results for $F_+^{\pi\pi\pi^0}$ and $F_+^{KK\pi^0}$ for each tag category, and combined. The *CP*-eigenstate tag results are from Ref. [1]. When two uncertainties are shown, the first is statistical and the second systematic. For the combined result the total uncertainty is given.

Tag	$F_+^{\pi\pi\pi^0}$	$F_+^{KK\pi^0}$
CP eigenstates	$0.968 \pm 0.017 \pm 0.006$	$0.731 \pm 0.058 \pm 0.021$
$K^0_{\rm S,L}\pi^+\pi^-$	$1.014 \pm 0.045 \pm 0.022$	$0.734 \pm 0.106 \pm 0.054$
Combined	0.973 ± 0.017	0.732 ± 0.055

measurement of the unitarity-triangle angle γ through the process $B^\mp \to DK^\pm$. The decays $D \to K^0_{\rm S,L}\pi^+\pi^-$ have also been employed as a tag to measure the *CP* contents of the modes $D \to \pi^+\pi^-\pi^0$ and $D \to K^+K^-\pi^0$. The results confirm the conclusion of an earlier analysis [1], based on *CP*-eigenstate tags, that the *CP*-even content of the $\pi^+\pi^-\pi^0$ final state is very high, and therefore this decay too is a powerful mode for the measurement of γ. Combining the two sets of measurements yields $F_+^{\pi\pi\pi^0} = 0.973 \pm 0.017$ and $F_+^{KK\pi^0} = 0.732 \pm 0.055$. Now that their *CP*-even fractions have been measured, all three decay modes may also be used for studies of indirect *CP* violation and mixing in the $D^0\overline{D}^0$ system [5].

Acknowledgments

This analysis was performed using CLEO-c data, and as members of the former CLEO collaboration we thank it for this privilege. We are grateful for support from the UK Science and Technology Facilities Council and the UK-India Education and Research Initiative.

References

[1] M. Nayak *et al.*, *First determination of the CP content of $D \to \pi^+\pi^-\pi^0$ and $D \to K^+K^-\pi^0$*, Phys. Lett. **B 740** (2015) 1, arXiv:1410.3964 [hep-ex].

[2] K.A. Olive *et al.* (Particle Data Group), *Review of particle physics*, Chin. Phys. **C 38** (2014) 090001.

[3] R. Aaij *et al.* (LHCb collaboration), *A model-independent unbinned search for CP violation in $D^0 \to \pi^+\pi^-\pi^0$ decays*, Phys. Lett. **B 740** (2015) 158, arXiv:1410.4170 [hep-ex].

[4] R. Aaij *et al.* (LHCb collaboration), *Model-independent search for CP violation in $D^0 \to K^-K^+\pi^-\pi^+$ and $D^0 \to \pi^-\pi^+\pi^-\pi^+$ decays*, Phys. Lett. **B 726** (2013) 623, arXiv:1308.3189 [hep-ex].

[5] S. Malde, C. Thomas and G. Wilkinson, *Measuring CP violation and mixing in charm with inclusive self-conjugate multibody decay modes*, arXiv:1502.04560 [hep-ph].

[6] A. Bondar and A. Poluektov, *The use of quantum correlated D^0 decays for ϕ_3 measurements*, Eur. Phys. J. **C 55** (2008) 51, arXiv:0801.0840 [hep-ex].

[7] M. Gronau and D. London, *How to determine all the angles of the unitarity triangle from $B^0_d \to DK_S$ and $B^0_s \to D\phi$*, Phys. Lett. **B 253** (1991) 483; M. Gronau and D. Wyler, *On determining a weak phase from CP asymmetries in charged B decays*, Phys. Lett. **B 265** (1991) 172.

[8] Y. Kubota *et al.* (CLEO collaboration), *The CLEO II detector*, Nucl. Instrum. Meth. **A 320** (1992) 66; D. Peterson *et al.*, *The CLEO III drift chamber*, Nucl. Instrum. Meth. **A 478** (2002) 142; M. Artuso *et al.*, *Construction, pattern recognition and performance of the CLEO III LiF-TEA RICH detector*, Nucl. Instrum. Meth. **A 502** (2003) 91; R.A. Briere *et al.* (CLEO-c/CESR-c Taskforces and CLEO-c collaboration), *CLEO-c and CESR-c: a new frontier of weak and strong interactions*, Cornell LEPP Report CLNS Report No. 01/1742 (2001).

[9] D.J. Lange, *The EvtGen particle decay simulation package*, Nucl. Instrum. Meth. **A 462** (2001) 152.

[10] R. Brun *et al.*, GEANT 3.21, CERN Program Library Long Writeup W5013, unpublished.

[11] D.M. Asner *et al.* (CLEO collaboration), *Determination of the* $D^0 \to K^+\pi^-$ *relative strong phase using quantum-correlated measurements in* $e^+e^- \to D^0\bar{D}^0$ *at CLEO*, Phys. Rev. **D 78** (2008) 012001, arXiv:0802.2268 [hep-ex].

[12] N. Lowrey *et al.* (CLEO collaboration), *Determination of the* $D^0 \to K^-\pi^+\pi^0$ *and* $D^0 \to K^-\pi^+\pi^+\pi^-$ *coherence factors and average strong-phase differences using quantum-correlated measurements*, Phys. Rev. **D 80** (2009) 031105(R), arXiv:0903.4853 [hep-ex].

[13] J. Libby *et al.*, *New determination of the* $D^0 \to K^-\pi^+\pi^0$ *and* $D^0 \to K^-\pi^+\pi^+\pi^-$ *coherence factors and average strong-phase differences*, Phys. Lett. **B 731** (2014) 197, arXiv:1401.1904 [hep-ex].

[14] H. Albrecht *et al.* (ARGUS collaboration), *Search for hadronic* $b \to u$ *decays*, Phys. Lett. **B 241** (1990) 278.

[15] T. Skwarnicki, *A Study of the radiative cascade transitions between the* Υ *and* Υ' *resonances*, Ph.D Thesis (Appendix E), Cracow, INP (1986), DESY F31-86-02.

[16] Q. He *et al.* (CLEO collaboration), *Comparison of* $D \to K^0_S\pi$ *and* $D \to K^0_L\pi$ *Decay Rates*, Phys. Rev. Lett. **100** (2008) 091801, arXiv:0711.1463 [hep-ex].

[17] Y. Amhis *et al.* (HFAG), *Averages of b-hadron, c-hadron, and* τ*-lepton properties as of summer 2014*, arXiv:1412.7515, online updates at http://www.slac.stanford.edu/xorg/hfag.

[18] J. Libby *et al.* (CLEO collaboration), *Model-independent determination of the strong-phase difference between the decays* D^0 *and* $\bar{D}^0 \to K^0_{S,L}h^+h^-$ $(h = \pi, K)$ *and its impact on the measurement of the CKM angle* γ, Phys. Rev. **D 82** (2010) 112006, arXiv:1010.2817 [hep-ex].

[19] B. Aubert *et al.* (BaBar collaboration), *Improved measurement of the CKM angle γ in $B^{\mp} \to D^{(*)}K^{(*)\mp}$ decays with a Dalitz plot analysis of D decays to $K^0_S\pi^+\pi^-$ and $K^0_S K^+K^-$*, Phys. Rev. **D 78** (2008) 034023., arXiv:0804.2089 [hep-ex].

[20] P. del Amo Sanchez *et al.* (BaBar collaboration), *Evidence for direct CP violation in the measurement of the CKM angle γ with $B^{\mp} \to D^{(*)}K^{(*)\mp}$ decays*, Phys. Rev. Lett. **105** (2010) 121801, arXiv:1005.1096 [hep-ex].

[21] A. Poluektov *et al.* (Belle collaboration), *Evidence for direct CP violation in the decay $B \to D^{(*)}K$, $D \to K^0_S\pi^+\pi^-$ and measurement of the CKM phase ϕ_3*, Phys. Rev. **D 81** (2010) 112002, arXiv:1003.3360 [hep-ex].

[22] B. Aubert *et al.* (BaBar collaboration), *Measurement of the Cabibbo-Kobayashi-Maskawa angle γ in $B^{\mp} \to D^{(*)}K^{\mp}$ decays with a Dalitz analysis of $D^0 \to K^0_S\pi^-\pi^+$*, Phys. Rev. Lett. **95** (2005) 121802, arXiv:hep-ex/0504039.

[23] S. Brisbane, *CLEO-c $D \to K^0_{S/L}\pi^+\pi^-$ binned Dalitz-plot analyses optimised for CKM angle γ measurement and the commissioning of the LHCb front-end electronics*, DPhil Thesis (Chapter 3), University of Oxford (2010), CERN-THESIS-2010-206.